Journal of Biomedical Optics

BiomedicalOptics.SPIEDigitalLibrary.org

Transient increase in systemic interferences in the superficial layer and its influence on event-related motor tasks: a functional near-infrared spectroscopy study

Isao Nambu
Takuya Ozawa
Takanori Sato
Takatsugu Aihara
Yusuke Fujiwara
Yohei Otaka
Rieko Osu
Jun Izawa
Yasuhiro Wada

SPIE.

Isao Nambu, Takuya Ozawa, Takanori Sato, Takatsugu Aihara, Yusuke Fujiwara, Yohei Otaka, Rieko Osu, Jun Izawa, Yasuhiro Wada, "Transient increase in systemic interferences in the superficial layer and its influence on event-related motor tasks: a functional near-infrared spectroscopy study," *J. Biomed. Opt.* **22**(3), 035008 (2017), doi: 10.1117/1.JBO.22.3.035008.

Journal of Biomedical Optics 22(3), 035008 (March 2017)

Transient increase in systemic interferences in the superficial layer and its influence on event-related motor tasks: a functional near-infrared spectroscopy study

Isao Nambu,[a,*,†] Takuya Ozawa,[a,b,†] Takanori Sato,[a] Takatsugu Aihara,[b] Yusuke Fujiwara,[b] Yohei Otaka,[b,c,d] Rieko Osu,[b] Jun Izawa,[b,e] and Yasuhiro Wada[a]
[a]Nagaoka University of Technology, Graduate School of Engineering, Nagaoka, Japan
[b]ATR Brain Information Communication Research Lab Group, Keihanna-Science City, Kyoto, Japan
[c]Tokyo Bay Rehabilitation Hospital, Narashino, Chiba, Japan
[d]Keio University School of Medicine, Department of Rehabilitation Medicine, Shinjuku-ku, Tokyo, Japan
[e]University of Tsukuba, Faculty of Engineering, Information and System, Tsukuba, Ibaraki, Japan

Abstract. Functional near-infrared spectroscopy (fNIRS) is a widely utilized neuroimaging tool in fundamental neuroscience research and clinical investigation. Previous research has revealed that task-evoked systemic artifacts mainly originating from the superficial-tissue may preclude the identification of cerebral activation during a given task. We examined the influence of such artifacts on event-related brain activity during a brisk squeezing movement. We estimated task-evoked superficial-tissue hemodynamics from short source–detector distance channels (15 mm) by applying principal component analysis. The estimated superficial-tissue hemodynamics exhibited temporal profiles similar to the canonical cerebral hemodynamic model. Importantly, this task-evoked profile was also observed in data from a block design motor experiment, suggesting a transient increase in superficial-tissue hemodynamics occurs following motor behavior, irrespective of task design. We also confirmed that estimation of event-related cerebral hemodynamics was improved by a simple superficial-tissue hemodynamic artifact removal process using 15-mm short distance channels, compared to the results when no artifact removal was applied. Thus, our results elucidate task design-independent characteristics of superficial-tissue hemodynamics and highlight the need for the application of superficial-tissue hemodynamic artifact removal methods when analyzing fNIRS data obtained during event-related motor tasks. [DOI: 10.1117/1.JBO.22.3.035008]

Keywords: functional near-infrared spectroscopy; event-related design; superficial-tissue hemodynamics; artifact removal; general linear model.

Paper 160693RR received Oct. 6, 2016; accepted for publication Feb. 24, 2017; published online Mar. 15, 2017.

1 Introduction

Functional near-infrared spectroscopy (fNIRS) is a noninvasive neuroimaging technique capable of measuring changes in the concentration of oxygenated and deoxygenated hemoglobin (ΔOxy-Hb and ΔDeoxy-Hb) in the cerebrovascular system based upon changes in the absorption of near-infrared light in the cerebral cortex.[1–5] Most previous studies of motor tasks have utilized the "block design" paradigm, wherein participants repeatedly perform a series of movements for several seconds, in order to detect movement-related changes in hemoglobin concentration using fNIRS.[6–10] Another type of task design, the "event-related design," has recently become popular in fNIRS studies.[11–18] In event-related tasks, participants perform the movement or task only once per trial, which usually occurs within 1 s. The cerebral activity evoked by this brief event is then identified. Such event-related task designs are common in other types of neuroimaging, such as functional magnetic resonance imaging (fMRI)[19,20] or electroencephalography (EEG).[12,17,21] This experimental design has no constraints on the task setting and allows one to evaluate cerebral activity for single (short duration) motor events or cognitive processes (e.g., quick motor responses to an event or movement preparation), which are usually difficult to observe in a block design paradigm. In addition, event-related designs are more easily applied in a variety of real life environments and clinical scenarios when compared to block designs. They can also be used in combined fNIRS and EEG studies for the detection of event-related responses.[12,17,21]

Recent studies have revealed that fNIRS signals reflect not only cerebral activity, but also systemic changes originating from both cerebral and superficial (scalp) layers.[5,22–27] Systemic changes in the superficial (scalp) layer, which are referred to as superficial-tissue hemodynamics (scalp hemodynamics), are thought to be especially problematic because they increase in a task-related manner and may obscure movement-related cerebral activity. A number of artifact removal methods have been proposed for the reduction of interference due to superficial-tissue hemodynamic artifacts and have been validated in block design tasks[6,24,28–34] as well as in real-time methods,[30,35,36]

*Address all correspondence to: Isao Nambu, E-mail: inambu@vos.nagaokaut.ac.jp

†These authors contributed equally to this article.

although methods used for the reduction of superficial-tissue hemodynamic artifacts during event-related tasks have not yet been well examined.[18,23] In a previous study, Minati et al.[23] observed that ballistic event-related motor tasks (e.g., arm raising) evoke global systemic changes in the superficial-tissue hemodynamic artifacts of fNIRS data from the visual cortex, even though this region was unrelated to the task. Another study by Scarpa et al.[18] has revealed that a superficial-tissue hemodynamic artifact removal method using 5-mm probe distance channels as references can improve the detection of cerebral activity during event-related motor tasks. However, no study has examined the temporal profiles of superficial-tissue hemodynamic artifacts directly over sensorimotor areas during event-related motor tasks. In addition, it remains unclear whether removal of superficial-tissue hemodynamic artifacts in event-related tasks is possible using other artifact removal methods that have been used for block design data.[6,25,28–36] During event-related motor tasks, superficial-tissue hemodynamic artifacts may hinder the detection of cerebral activity more significantly than they do during block design tasks. This is due to the small amplitude of cerebral activity in event-related motor tasks.[18] For this reason, it is necessary to empirically examine the characteristics of superficial-tissue hemodynamic artifacts over the sensorimotor cortex, as well as the applicability of various removal methods during event-related motor tasks.

The primary purpose of this study was to examine the characteristics of superficial-tissue hemodynamic artifacts related to a single motor event. We conducted an event-related motor experiment (exp. 1), in which fNIRS data were collected using 15-mm probe (source and detector) distance channels (referred to as short channels) and 30-mm standard-distance channels. We then extracted global superficial-tissue hemodynamics from data measured by the short channels using principle component analysis (PCA). The use of short channels (distances of ≤ 15 mm) is known to be effective because the signals measured primarily reflect changes in superficial (scalp) layers, whereas signals obtained from standard-distance channels reflect the hemodynamics of both the cerebral and scalp layers.[6,26] In order to elucidate the characteristics of superficial-tissue hemodynamics in an event-related design, we also performed the same analysis on data during a block design task (exp. 2) and compared the temporal profiles of superficial-tissue hemodynamic artifacts. To our knowledge, no such comparison between different task designs has been made before.

In addition, we examined the effectiveness of a previously proposed removal method that estimates brain activity using a general linear model (GLM) with 15-mm short channels.[6] This method is different from the method used in the previous study (Scarpa et al.[18]) but has been shown to be effective in block design motor tasks.[6] This method is simple and easy-to-use and relies on a PCA algorithm for the processing of data from 15-mm probe distance channels, which can be easily measured by allocating the probes in the middle of the standard probe pairs in commercially available systems.[6,31] In order to confirm previous findings that have indicated the importance of superficial-tissue hemodynamic artifact removal for event-related task designs,[18] we evaluated the effectiveness of this method in the event-related motor tasks of this study by comparing results obtained with and without application of superficial-tissue hemodynamic artifact removal methods.

2 Methods

2.1 *Participants*

Two experiments (exp. 1 and exp. 2) were conducted according to the guidelines outlined within the declaration of Helsinki and were approved by the ATR Human Subject Review Committee and the Institutional Ethical Committee of Nagaoka University of Technology. Eighteen healthy, right-handed participants (P1 to 18, fourteen men, mean age: 37.6 years) took part in the experiment. In each experiment, data were collected from eleven participants (P1 to 11, eight men, mean age: 45.6 years for exp. 1; P8 to 18, 10 men, mean age: 24.5 years for exp. 2). Five participants (P7 to 11) took part in both exp. 1 and exp. 2. All participants provided written informed consent prior to participation in the experiments.

2.2 *Experimental Procedures*

2.2.1 *Event-related design experiment (exp. 1)*

We adopted an event-related design for exp. 1, which utilized a brisk ball-grasping task. Participants were asked to remain relaxed while seated in a chair and hold a plastic ball in either their left or right hand. They were asked to avoid movements not related to the task while gazing at a fixation point during the experiment. About 1 s after a cue beep (1 kHz) was heard from a personal computer, the participants were asked to quickly squeeze and release the plastic ball [Fig. 1(a)]. The cue beep was presented using a random interval of 5 to 15 s in length (mean: 10 s, uniformly distributed), so that the participants were not able to predict the cue timing. A single trial was defined as one grasping movement following the cue beep, with each session consisting of 20 trials. To detect the timing of the grasping event in a trial, we recorded ball pressure levels using a custom-made pressure sensor for five participants (P1 to 5). For the remaining participants (P6 to 11), we recorded muscle activity of the brachioradialis using an electromyography sensor (Trigno, Delsys Inc., Natick, Massachusetts) to detect the event. The event onset was defined as the time when the pressure level or muscle activity exceeded the mean of the value over the course of the session. A 10-s rest period was included at the beginning of each session for baseline correction. Five out of the 11 participants (P1 to 5) completed the experimental sessions over a 2-day period, performing 10 sessions/day for each hand. Thus, a total of 200 trials were performed for each hand. The remaining participants (P6 to 11) completed the experimental sessions with both the left and right hands in a single day, performing a total of five sessions for each hand (10 sessions/day). Thus, a total of 100 trials were performed for each hand. One participant (P7) completed only four sessions for each hand due to scalp pain. We assumed that the data obtained from the left- and right-hand tasks for each participant were independent and analyzed each as a separate sample, as assumed in previous studies.[6,8] Thus, a total of 22 samples (11 participants $\times$ 2 hands) were obtained for exp. 1.

2.2.2 *Block design experiment (exp. 2)*

A block design paradigm[6–10] was adopted for exp. 2, which utilized the same ball-grasping task as exp. 1. In each block design trial, the cue beep (1 kHz) was presented to the participant at the start and end of the 10-s task period. Approximately 1 s after the initial cue beep was presented, the participant was required to

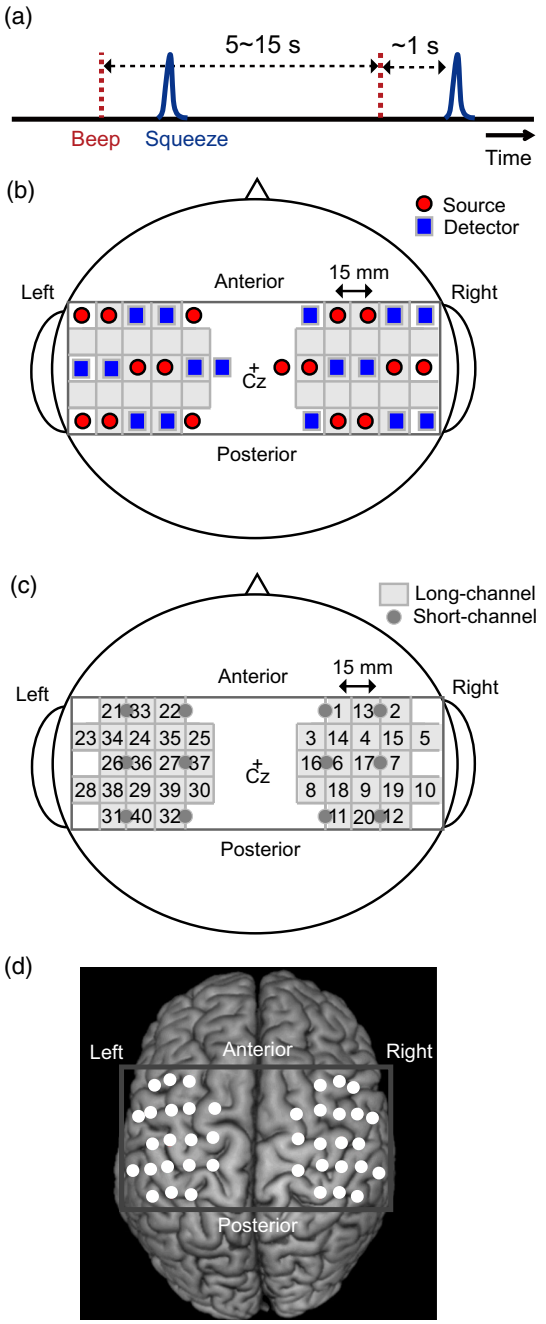

Fig. 1 Experimental setting. (a) Task timing in exp. 1. Around 1 s after the beep, the participant was required to squeeze the ball one time. The intertrial interval was randomized from 5 to 15 s. (b) Probe positions. Sixteen sources (red circles) and 16 detectors (blue rectangles) were placed over bilateral sensorimotor areas with double density arrangements.[37] (c) Channel positions. Data were measured from 40 long channels and 12 short channels covering the bilateral sensorimotor areas. Due to the double-density arrangement, the distance between two long channels was 15 mm. (d) Channel positions projected onto the standard brain image. White circles indicate each long-channel position. The image was created using MRIcron software.

squeeze the ball repeatedly (10 times) under the guidance of a cue beep (500 Hz sine wave) presented at a frequency of 1 Hz. Random intertrial intervals of 10 to 12 s were used (uniformly distributed). Each session consisted of 10 trials, and a total of five sessions were conducted for each hand. The experiment was conducted for both hands in a single day, resulting in a total of 100 trials (50 trials for each hand). As in exp. 1, we assumed that the left and right-hand datasets were independent (see Sec. 2.2.1) and evaluated a total of 22 samples from exp. 2.

2.3 *Measurement of Functional Near-Infrared Spectroscopy Signals*

We used a multichannel fNIRS system (FOIRE-3000, Shimadzu Corp., Kyoto, Japan; wavelengths: 780, 805, and 830 nm). The sampling period was 130 ms. The fNIRS probes (i.e., source and detector) were placed around Cz of the international 10 to 20 system to cover the sensorimotor cortex of both hemispheres [Fig. 1(b)]. This probe arrangement consisted of 40 standard 30-mm probe distance channels (long channels) and 12 shorter probe distance channels (15 mm, short channels) [Fig. 1(c)]. In order to improve the spatial resolution of the fNIRS measurement, we set the long channels at double the density[37] of the standard arrangement [Fig. 1(c)]. Following the fNIRS experiments, probe positions were measured using a stylus marker (FASTRAK, Polhemus, Colchester, Vermont). The measured signals were converted to relative changes in hemoglobin concentration (ΔOxy-Hb and ΔDeoxy-Hb) according to a modified Beer–Lambert law.[1]

2.4 *Analysis*

2.4.1 *Preprocessing*

All analyses were performed using MATLAB (Mathworks Inc., Natick, Massachusetts). The fNIRS signal was smoothed using a Butterworth low-pass filter (fourth-order, cutoff frequency: 0.7 Hz) in order to remove high-frequency components derived from physiological factors such as heart rate. Furthermore, a discrete cosine transform with a cutoff frequency of 0.02 Hz was used for high-pass filtering to eliminate very-low-frequency trend components. Baseline correction was performed by converting the mean value during the 10-s rest period to zero. Data from channels whose standard deviations after preprocessing were extremely large (>0.01 mMcm) and data from trials during which substantial body movement was observed were excluded from further analysis. The average number of excluded trials across the samples was 1.9. The averaged probe positions in Montreal Neurological Institute (MNI) coordinates across participants were calculated using the NFRI function toolbox[38] and mapped to the standard brain [Fig. 1(d)].

2.4.2 *Estimation of superficial-tissue hemodynamic artifacts*

As previously noted, fNIRS signals (ΔOxy-Hb and ΔDeoxy-Hb) include global systemic changes in the superficial layer (superficial-tissue hemodynamic artifact) as a result of the principle of the measurement itself.[5,27] Here we estimated global superficial-tissue hemodynamic artifacts using the method proposed by Sato et al.[6] In this method, the superficial-tissue hemodynamics is estimated using PCA of the preprocessed short-channel signals. We defined the principal component that had the highest contribution ratio (variance accounted for) as that representing global superficial-tissue hemodynamics. The short-channel data were normalized (z-scored) before performing the PCA. This superficial-tissue hemodynamic artifact estimation procedure was performed for both ΔOxy-Hb and ΔDeoxy-Hb signals.

To examine the characteristics of the estimated superficial-tissue hemodynamic artifact in the event-related design, we calculated the average superficial-tissue hemodynamics across samples in exp. 1. We then calculated the correlation coefficients ($r_{\text{cereb-superficial}}$) between the average superficial-tissue hemodynamics and the cerebral hemodynamic model. The cerebral hemodynamic model was derived by convoluting the canonical hemodynamic response function[39] and the delta function at the start of the grasping movement from ball pressure or muscle activity. We also evaluated the peak latency, which represents the time at which fNIRS signals exhibit maximum amplitude, from movement onset for both cerebral and superficial-tissue hemodynamics. The same analysis for short channels was applied to the data in the block design (exp. 2), and average scalp and cerebral hemodynamics for both experiments were compared.

2.4.3 *Estimation of brain activity using general linear model*

To estimate cerebral activity and remove superficial-tissue hemodynamic artifacts for the event-related design (exp. 1), we analyzed the data using a GLM known as ShortPCA[6] for the reduction of superficial-tissue hemodynamic artifacts. In this model, the measured fNIRS hemoglobin signal Y is represented as a linear combination of the design matrix, as

$$Y = \mathbf{X}_c\boldsymbol{\beta}_c + \mathbf{X}_s\boldsymbol{\beta}_s + \mathbf{X}_{\text{const}}\boldsymbol{\beta}_{\text{const}} + \boldsymbol{\varepsilon}, \quad (1)$$

where $\mathbf{X}_c$, $\mathbf{X}_s$, and $\mathbf{X}_{\text{const}}$ represent the design matrices aligned for each session, and $\boldsymbol{\beta}_c$, $\boldsymbol{\beta}_s$, and $\boldsymbol{\beta}_{\text{const}}$ represent the regression coefficients for the cerebral, superficial-tissue, and constant terms, respectively. The term $\mathbf{X}_c$ consists of the cerebral hemodynamic model (see above, Sec. 2.4.2) and its first and second derivatives. The estimated superficial-tissue hemodynamics from short channels (Sec. 2.4.2) was represented using $\mathbf{X}_s$. $\mathbf{X}_{\text{const}}$, is a vector whose components each had a value of 1. The term $\boldsymbol{\varepsilon}$ is a residual component that follows a normal distribution with zero mean and variance σ^2.

We conducted first-level analysis using the GLM for each sample. We estimated beta values ($\hat{\boldsymbol{\beta}}_c$, $\hat{\boldsymbol{\beta}}_s$, and $\hat{\boldsymbol{\beta}}_{\text{const}}$) using the ordinary least squares method to minimize $\boldsymbol{\varepsilon}$. By determining $\hat{\boldsymbol{\beta}}_c$, estimates of cerebral hemodynamics were obtained as $\mathbf{X}_c\hat{\boldsymbol{\beta}}_c$. We then evaluated the estimates of the cerebral hemodynamics using the average laterality index (LI)[40] of the t-values. Research has established that hand or finger movements induce brain activity in the sensorimotor areas contralateral to those for the moving hand,[41] and that the LI represents such predominance of the contralateral activation. To this end, we calculated the t-value for each sample (i.e., sample-wise t-value[6,39]), which was obtained by dividing $\hat{\beta}_c$ by the standard deviation σ^2 of the residuals to account for the influence of the signal-to-noise ratio (SNR). We used the precoloring method to correct for serial correlation in the residuals.[6,39,42] The LI for each sample was calculated as follows using the obtained t-values:[40]

$$\text{LI} = (Q_{\text{Contra}} - Q_{\text{Ipsi}})/(|Q_{\text{Contra}}| + |Q_{\text{Ipsi}}|), \quad (2)$$

where Q_{Contra} and Q_{Ipsi} represent the sums of the t-values in each channel in the hemispheres contralateral and ipsilateral to the grasping hand, respectively. To examine the effects of superficial-tissue hemodynamic artifact removal on the detection of event-related motor activity, we also calculated t-values and LIs using the GLM model without superficial-tissue hemodynamic artifact removal [i.e., $\mathbf{X}_s\boldsymbol{\beta}_s$ was not used in Eq. (1)], which is referred to as RAW. We then compared the LIs obtained using ShortPCA and RAW by performing a one-sample t-test. For comparison, we also calculated LIs obtained using ShortPCA for the block design experiment (exp. 2).

Next, we performed group-level analysis (second-level)[13] in order to examine the cerebral activation maps across samples. In this analysis, group-level t-values for each channel were calculated for $\hat{\beta}_c$ (of samples) using a one-sample t-test. This analysis was performed separately for each hand. Note that group-level t-values were obtained for each channel, while sample-wise t-values were obtained for each sample and channel (i.e., total 22 t-values for each channel). We used a multiple comparison test accounting for false discovery rate (FDR_{BH})[43] and evaluated the resulting p-values to determine statistical significance (FDR q level = 0.05).

3 Results

3.1 *Estimated Superficial-Tissue Hemodynamic Artifacts in the Event-Related Motor Task*

Using data obtained from short channels, we estimated global superficial-tissue hemodynamics for ΔOxy-Hb and ΔDeoxy-Hb [Fig. 2(a)] in exp. 1. Increases in both hemoglobin signals were observed from the onset of movement, which peaked at ~4 to 5 s (average: 4.38 s; Table 1). When we conducted the same analysis for the block design experiment (exp. 2), the global superficial-tissue hemodynamics similarly increased from the onset of movement, peaking at around 5 s [Fig. 2(b)]. We then compared the superficial-tissue hemodynamic data obtained from exp. 1 (event-related design) with that obtained in exp. 2 (block design) and with the cerebral hemodynamic model (i.e., cerebral activity) in order to examine the characteristics of the estimated global superficial-tissue hemodynamics. Despite different experimental designs, the global superficial-tissue hemodynamics for both event-related and block design tasks exhibited similar task-related increases. Furthermore, both resembled the cerebral hemodynamics of the event-related design [Fig. 2(c)]. However, peak cerebral hemodynamic values in the block experiment were observed 11 s after the onset, while peak latencies for superficial-tissue hemodynamics in the event-related and block-design were ~5 s after onset of movement (Table 1). Averaged global superficial-tissue hemodynamics was highly correlated with averaged cerebral hemodynamics in the event-related tasks, though low correlation was observed for the block design task ($r_{\text{cereb-superficial}}$; Table 1).

3.2 *Brain Activity with Superficial-Tissue Hemodynamic Artifacts*

3.2.1 *Individual analysis (single-sample level)*

Figure 3 shows an example of the event-triggered averages for measured estimated superficial-tissue and cerebral hemodynamics in a representative participant. Superficial-tissue hemodynamics [red line in Fig. 3(a)] was observed across measured channels while increases in cerebral hemodynamics of ΔOxy-Hb were found in the contralateral (left) sensorimotor channels [black line, Fig. 3(a)]. Superficial-tissue hemodynamics of ΔDeoxy-Hb was subtle [Fig. 3(b)]. Next, we evaluated cerebral activity for each sample using GLM analysis. Figure 4(a) shows data from a representative participant.

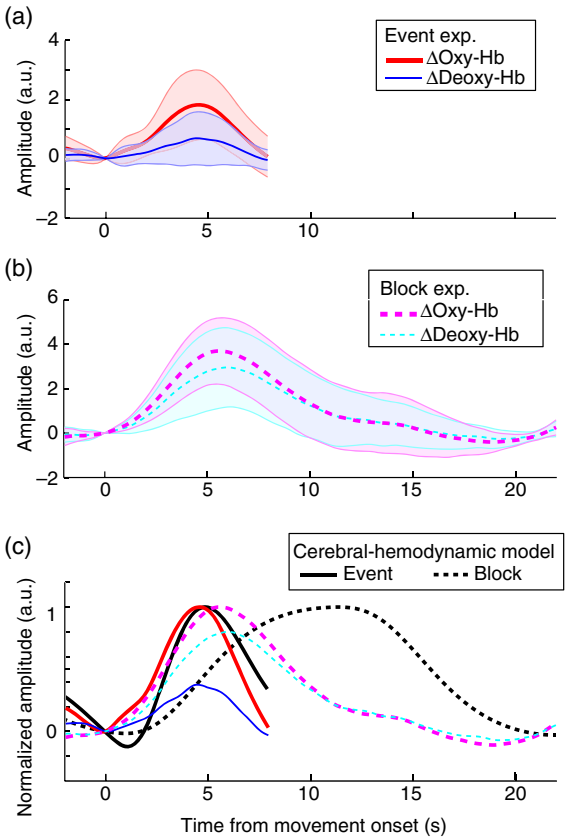

Fig. 2 Superficial-tissue hemodynamic signals extracted from short channels. (a) Average superficial-tissue hemodynamics across samples for the event-related experiment. The bold red line represents ΔOxy-Hb, while the thin blue line represents ΔDeoxy-Hb. Shaded areas represent the standard deviation for each sample. The data for 8 s after movement onset are shown due to the minimal rest period included at the end of each session (i.e., duration after the final motor task in the session) was 8 s. Amplitude (vertical axis) is arbitrary unit (a.u.) because the superficial-tissue hemodynamic signals were extracted after applying PCA to normalized (z-scored) short-channel data. (b) Average superficial-tissue hemodynamics across samples for the block design experiment. Bold magenta and thin cyan lines represent ΔOxy-Hb and ΔDeoxy-Hb, respectively. Shaded areas represent the standard deviation for each dataset. (c) Comparison of the cerebral- and superficial-tissue hemodynamics between the experiments. The bold and thin black lines represent the cerebral-hemodynamic models for the event-related and block design experiments, respectively. Note that each amplitude was normalized so that the maximum amplitude of the superficial-tissue hemodynamics for ΔOxy-Hb in each task was 1.

Broad activation was detected without removal of superficial-tissue hemodynamic artifacts (RAW), especially for ΔOxy-Hb [Fig. 4(a), upper left]. Because strong activation is expected in the contralateral areas to the moving hand or fingers, our results suggest that false-positive activation occurred in the ipsilateral hemisphere. Using the GLM analysis that incorporated the removal of superficial-tissue hemodynamic artifacts (ShortPCA), activation in the ipsilateral hemisphere was suppressed, and the LI was increased for ΔOxy-Hb (e.g., LI was 0.44 for ShortPCA and 0.10 for RAW; Fig. 4(a), lower left). The LI for ShortPCA was significantly increased relative to that for RAW data [0.33 for ShortPCA and 0.27 for RAW; $t[21] = 2.31$, $p < 0.05$; Fig. 4(b)]. In contrast, results for ΔDeoxy-Hb were nearly identical, and no significant LI difference was observed [Fig. 4(a), right]. The mean LIs obtained using ShortPCA for block design data (exp. 2) were 0.24 for ΔOxy-Hb and −0.20 for ΔDeoxy-Hb.

Table 1 Characteristics of the extracted superficial-tissue hemodynamic artifacts.

		$r_{\text{cereb-superficial}}$ (±SD)	Mean first PC contribution ratio (±SD)	Mean peak latency (s) (±SD)
Superficial-tissue hemodynamics				
ΔOxy-Hb	Event	0.64 (±0.37)	0.65 (±0.13)	4.38 (±1.57)
	Block	0.29 (±0.37)	0.81 (±0.09)	5.75 (±0.73)
ΔDeoxy-Hb	Event	0.37 (±0.55)	0.32 (±0.08)	3.39 (±2.80)
	Block	0.33 (±0.34)	0.68 (±0.26)	6.46 (±1.82)
Cerebral hemodynamics				
	Event			4.93 (±0.03)
	Block			11.33 (±0.31)

Note: PC: principal component; SD: standard deviation.

3.2.2 *Group-level analysis*

Group-level analysis of RAW data revealed no significant increases in ΔOxy-Hb during the right-hand task [Fig. 4(c), upper left]. We also found activation in the ipsilateral hemisphere during the left-hand task [Fig. 4(d), upper left]. Such differences may be due to individual differences in the patterns of activation evoked by movements of the left and right hands. Similar to the results obtained during the individual analysis, ShortPCA improved lateralization in the activation map of ΔOxy-Hb for both tasks [Figs. 4(c) and 4(d), lower left]. The corresponding LIs were increased (from 0.47 to 0.60 for the right hand, and from 0.23 to 0.29 for the left hand). However, no improvements in ΔDeoxy-Hb were observed. In fact, there was deterioration of the right-hand data [right in Figs. 4(c) and 4(d)].

4 Discussion

In this study, we investigated the characteristics of superficial-tissue hemodynamic components contained in fNIRS signals obtained from participants engaging in an event-related motor task. Our results indicate that the superficial-tissue hemodynamics in the event-related design as well as in the block design exhibited similar, task-related changes when compared with cerebral activity. Thus, the influence of superficial-tissue hemodynamics on the detection of event-related motor activity is likely to be substantial. The results of our GLM analysis support this hypothesis and further highlight the importance of superficial-tissue hemodynamic artifact removal.

4.1 *Characteristics of Superficial-Tissue Hemodynamics*

Analyses of signals from short channels (Fig. 2) revealed several characteristics of superficial-tissue hemodynamics. We

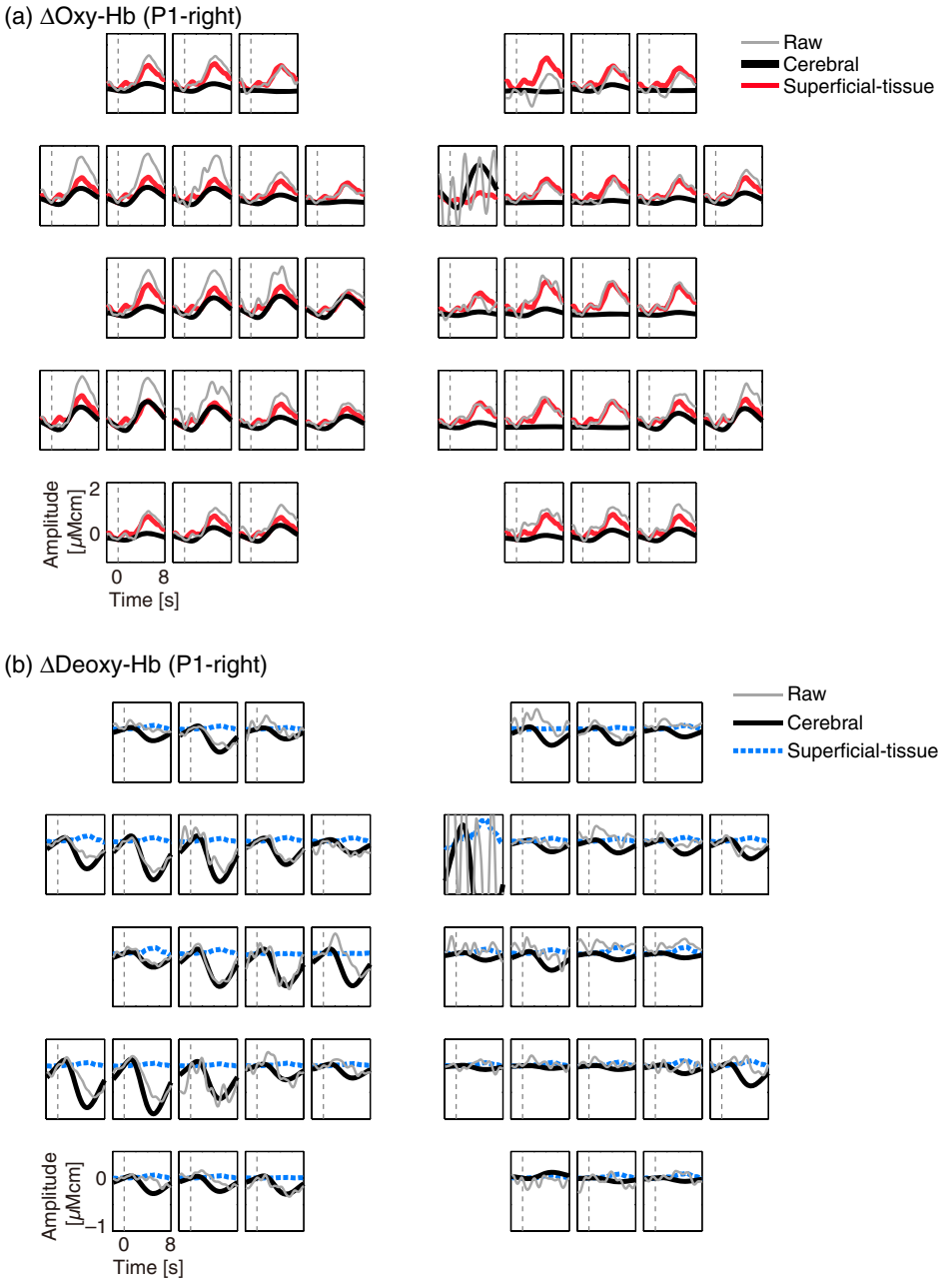

Fig. 3 Event-triggered averages. (a) ΔOxy-Hb and (b) ΔDeoxy-Hb for a representative participant (P1, right-hand task) are shown. Gray thin lines represent measured (raw) data. Black bold lines show cerebral hemodynamics estimated by GLM analysis. Red bold and blue dashed bold lines indicate estimated superficial-tissue hemodynamics for ΔOxy- and ΔDeoxy-Hb, respectively. Dashed vertical line represents task onset. Note that the scale of the vertical axis is different between (a) and (b).

observed that superficial-tissue hemodynamics changed in a task-related manner, peaking at ~5 s after the onset of movement (Table 1). This result aligns with those of a previous report, which found that an event-related motor task evoked transient increases in fNIRS signals in the visual cortex.[23] Our results indicate that such task-evoked increases are similarly observed in the sensorimotor areas.

Surprisingly, the temporal profiles of the superficial-tissue hemodynamics were closely matched in both the event-related and block design tasks. In the block design paradigm, cerebral activity is gradually increased and peaks at the end of the task duration [Fig. 2(c)] because the cerebral activity is assumed to be a linear function of task parameters.[39] Similar temporal changes are expected for superficial-tissue hemodynamics and cerebral activity in the block design task when superficial-tissue hemodynamics is also assumed to be dependent on task parameters (duration). Contrary to this expectation, in this study, the profile of superficial-tissue hemodynamics in the block design task was completely different from the cerebral hemodynamic profile and exhibited no relationship with task duration (i.e., no linearity). To examine whether this common transient increase in the systemic interferences is observed during other task designs, we collected fNIRS short-channel data during a motor task with different task durations (5-, 15- and

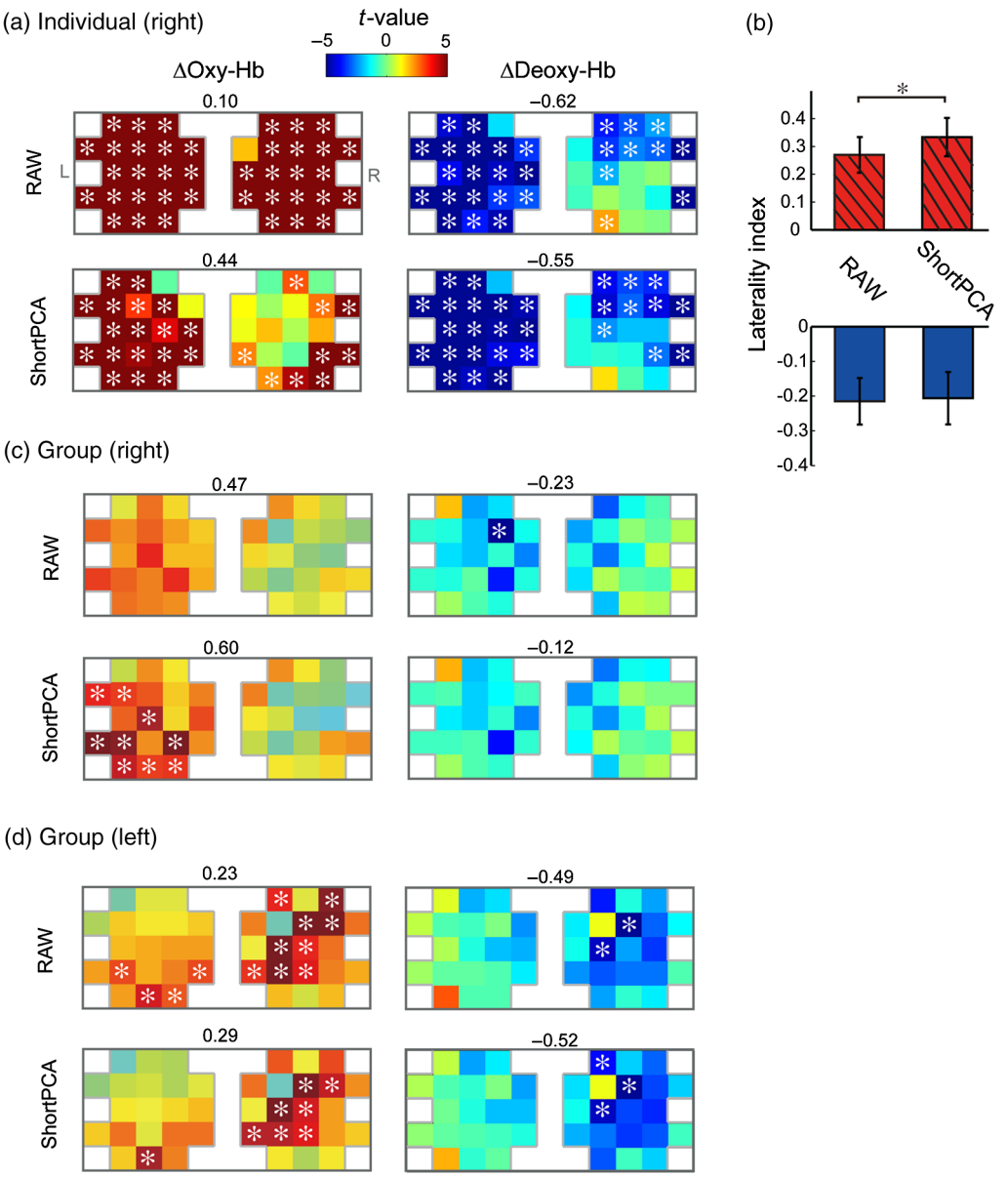

Fig. 4 Cerebral activation maps (t-maps) and laterality indices. (a) T-maps of RAW (top) and ShortPCA (bottom) analyses for ΔOxy-Hb (left) and ΔDeoxy-Hb (right) during the right-hand task of the representative participant (P1). Asterisks represent the channels for which statistically significant differences were observed ($p < 0.05$). Values above the map denote the LI. (b) Average LI across samples for ΔOxy-Hb (red, top) and ΔDeoxy-Hb (blue, bottom). The error bar represents the standard deviation. The asterisk represents statistical significance ($p < 0.05$). (c) Group-level t-maps for the right-hand task. (d) Group-level t-maps for the left-hand task.

30-s grasping) and a cognitive task [verbal fluency task (VFT)[44]]. We then analyzed superficial-tissue hemodynamics (Appendix A.1, data were partly presented previously[6]). Transient increases in superficial-tissue hemodynamics were observed across the analyzed datasets and peaked at ∼6 s, even when the task duration or the type of task differed (Appendix A.1.3 and Fig. 5). Similar superficial-tissue hemodynamic profiles have been consistently reported in previous studies.[6,31] In these reports, superficial-tissue hemodynamics first peaked at 5 to 6 s, increasing again after several seconds, although this rebound was relatively small for the block task in this study [Fig. 2(b)]. Thus, comparisons between event-related and block designs suggest that, at least for motor tasks, superficial-tissue hemodynamics consists of two components: a transient increase following onset, irrespective of task design, and a subsequent gradual increase dependent on task design (duration). The first component may represent the general characteristics of the superficial-tissue hemodynamics, and this "cerebral-hemodynamic-like" change may produce broad, false-positive activation and obscure the actual cerebral hemodynamic profile in event-related tasks.

However, the physiological origin of this transient superficial-tissue hemodynamic profile remains unclear. A number of authors have suggested that systemic changes in heart rate, respiration, and blood pressure are reflected in superficial-tissue hemodynamics.[5,22,25] Low-frequency oscillations (LFO) or

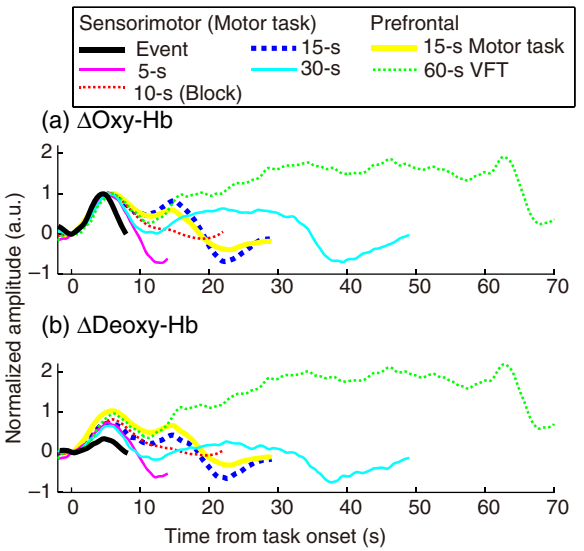

Fig. 5 Temporal profiles of superficial-tissue hemodynamics for different task designs. The data for (a) ΔOxy-Hb and (b) ΔDeoxy-Hb are shown. Each line represents data from a different design. The data for exp. 1 (event-related design) and exp. 2 (block design) in Fig. 2 are also shown using black bold and red thin lines, respectively. For illustration purposes, the amplitudes were normalized so that the peak value of ΔOxy-Hb from 0 to 10 s after task onset was 1.

Mayer waves are primary components of these signals, possibly reflecting changes in mean arterial blood pressures (MAP).[22] Changes in global superficial-tissue hemodynamics observed in this study (Fig. 2) occurred in cycles of ∼10 to 15 s (i.e., 0.06 to 0.1 Hz), which may reflect these LFO components. Thus, performance of motor tasks likely produce increases in MAP due to task-evoked vasodilation, following which such changes increase the magnitude or reset phases of LFOs, which eventually emerge in the superficial-tissue hemodynamics measured by short channels. Our results suggest that these changes in LFOs are independent of motor task parameters (e.g., duration, strength, and movement types). Such a notion is supported by the results of previous studies,[45,46] in which transient changes in arterial blood pressure (ABP) were observed during motor tasks, with first peaks occurring around 5 to 6 s after movement onset. Another study also revealed that cerebral blood volumes estimated from fNIRS hemoglobin signals (ΔOxy-Hb and ΔDeoxy-Hb), which are strongly influenced by ABP, exhibited task-locked temporal profiles.[47] Further studies are required in order to more fully examine such changes in a variety of experimental settings.

4.2 *Methods of Superficial-Tissue Hemodynamic Artifact Removal for Event-Related Motor Tasks*

The feasibility of superficial-tissue hemodynamic artifact removal has been confirmed for fNIRS data obtained during event-related motor tasks.[18] This previous method combines the estimation of the hemodynamic response and the removal of superficial-tissue hemodynamic artifacts using 5-mm probe distance (reference) channels. Here, we used another simple method of artifact removal using short-channel signals (15 mm) and GLM analysis (ShortPCA[6]). The use of the 15-mm short channels, however, represents one limitation of this method, as the signals from these channels may contain a small amount of cerebral hemodynamic information.[26] However, the influence of the cerebral hemodynamics can be subtle in ShortPCA, as it extracts and removes superficial-tissue hemodynamics globally distributed over the brain using PCA, while the task-related cerebral hemodynamics may be observed locally.[6] In addition, implementation and measurements of 15-mm short channels are easy to undertake (see Sec. 1). ShortPCA can thus be used for fNIRS measurements in broad areas, as previously indicated in studies utilizing block design tasks.[6] We found that ShortPCA can be used to identify event-related cerebral activity associated with ΔOxy-Hb during motor tasks, as indicated by an improvement in LI values [Fig. 4(b)]. Thus, consistent with the results obtained by Scarpa et al.,[18] our findings support the feasibility of superficial-tissue hemodynamic artifact removal methods for fNIRS data obtained during event-related tasks. In addition, we evaluated group-level spatial maps of cerebral activity [Figs. 4(c) and 4(d)] and found that removal of superficial-tissue hemodynamic artifacts is effective, even for group-level analyses. However, the influence of superficial-tissue hemodynamics was reduced to some extent by averaging across samples even when no method of superficial-tissue hemodynamic artifact removal was applied [Figs. 4(c) and 4(d)]. This suggests that the individual differences in superficial-tissue hemodynamics may be large. It is possible that such differences are eliminated by group-level analyses using large numbers of samples.[13,16]

4.3 *Limitations of this Study*

While our results support the feasibility of ShortPCA for detecting ΔOxy-Hb, this was not the case for ΔDeoxy-Hb. It is possible that ShortPCA fails to extract superficial-tissue hemodynamics in ΔDeoxy-Hb using short channels because the amplitudes of ΔDeoxy-Hb are relatively small, with low SNRs. ShortPCA assumes that the superficial-tissue hemodynamics are predominantly contained within short-channel signals and thus can be extracted using PCA, which identifies major components in the signals. Therefore, if SNR is low, the predominance of superficial-tissue hemodynamics is decreased, and PCA may extract local signals or other noise components. Indeed, when we evaluated SNRs for each of the hemoglobin signal,[34] we confirmed that SNR for ΔDeoxy-Hb was smaller than that for ΔOxy-Hb ($SNR_{\Delta Deoxy}/SNR_{\Delta Oxy}$ was 0.52, see Appendix A.2 for details), possibly because of individual differences in the sensitivity of ΔDeoxy-Hb. As a result, the contribution ratio of the first component extracted by PCA in ΔDeoxy-Hb was relatively small compared to that in ΔOxy-Hb (Table 1). Thus, ShortPCA may not be applicable when the SNR of the fNIRS signals is small.[6] It is also possible that ΔDeoxy-Hb does not contain superficial-tissue hemodynamic artifacts. A number of previous studies have reported that the effects of the artifact removal method are not observed for ΔDeoxy-Hb,[23,24,29,33,48,49] most likely due to the different origins (compartments) of ΔDeoxy-Hb and ΔOxy-Hb.

Among the superficial-tissue hemodynamic artifact removal methods proposed previously, we only tested ShortPCA for the removal of superficial-tissue hemodynamic artifacts, as this method is easily applicable to measurements of broad brain regions.[6] However, this method has several limitations. First, as discussed above, usage of 15-mm short channels may have a small risk of contamination by cerebral activity when one estimates superficial-tissue hemodynamics. Second, the method cannot reduce the effects of local systemic components

of superficial-tissue hemodynamics observed at some specific channels,[24,49–51] while it estimates and removes the global components. In addition, this method requires short-channel measurements and cannot be applied for data measured previously without short channels. Considering the cost of the short-channel measurements and their applicability, it may be better to use a method using long channels only. However, one should take care when applying the method using long channels, as it may have a risk of removing actual cerebral activity due to the similar temporal profiles between the cerebral and systemic components (Fig. 2).[23,24] Owing to its similarity, this could be problematic even when using short channels. As proposed by Zhang et al.,[33] taking the spatial natures of the systemic interferences into account may overcome this limitation. Our method also uses spatial information of the superficial-tissue hemodynamics by using multiple short channels located across measurement areas; this may reduce the risk of removing cerebral components to some extent.

The use of the long channels and the previously proposed systemic artifact removal methods using short channels may also be applicable to event-related designs, especially when using real-time adaptive algorithms.[30,35,36] Although comparisons of the existing artifact removal methods were beyond the scope of our study, it is of interest to conduct further research aimed at comparing the different methods, especially using simultaneous recordings of fNIRS and fMRI.[48] This may reveal the most effective and accurate way to investigate changes in cerebral activity during event-related motor tasks.

5 Conclusion

We analyzed signals from short channels using a 15-mm probe distance in order to investigate task-related superficial-tissue hemodynamics in both event-related and block design motor tasks. Our results indicate that such changes were task-design independent and resembled the cerebral hemodynamics observed during the event-related task. In addition, the results of our GLM analysis indicate that application of an artifact removal method to data obtained from short channels results in improved recognition of contralateral motor activity associated with ΔOxy-Hb. These results suggest that task design (event-related or block) substantially influences the detection of cerebral activity and further highlights the importance of applying superficial-tissue hemodynamic artifact removal methods, particularly when event-related paradigms are utilized.

Appendix A

A.1 *Superficial-Tissue Hemodynamics for Different Task Designs*

To examine whether transient increases in superficial-tissue hemodynamics (Fig. 2) are observed irrespective of task design, we collected five different datasets and compared estimated superficial-tissue hemodynamics from them. The datasets consisted of three measurements from bilateral sensorimotor areas during different motor tasks with varying durations (5, 15, and 30 s), and two measurements from prefrontal areas during motor and VFTs. Results using these datasets have partially been reported in a previous study.[6] All experiments were conducted according to guidelines outlined within the declaration of Helsinki and were approved by the institutional ethical committee of Nagaoka University of Technology. All participants provided written informed consent prior to participation in the experiments.

A.1.1 *Datasets for sensorimotor areas*

Three datasets obtained from bilateral sensorimotor areas were analyzed. Each dataset was measured during a grasping task with different durations (5, 15, and 30 s). The sampling period was 100 ms in all tasks, except for the 5-s task (85 ms).

In an experiment with a 5-s task, we measured data for 10 participants (mean age: 22.7 years) using 38 channels (34 long and 4 short). The channels covered the bilateral sensorimotor areas. For the purpose of the analysis, we only used short channels. We conducted a single session with 10 trials each for the left and right hands. A trial was defined as a 5-s grasping period and a 10-s resting period. Data for each hand from a single participant were regarded as an independent sample. Therefore, a total of 20 samples were analyzed.

The short-channel datasets used in the previous study (exp. 1 to 1)[6] were reanalyzed as 15-s task data. In this study, we used 20 samples (10 participants each for the left- and right-hand tasks; mean age: 23.4 years). The 18 short channels were located at bilateral sensorimotor areas. The detailed data are described in a previous study.[6]

We also collected another set of short-channel measurements during a 30-s motor task with the right hand. The same participants as those in the 15-s task were recruited (total of 10 samples). We used 18 short channels. In this task setting, a 30-s motor task and a 30-s rest period were repeated six times (total of six trials).

A.1.2 *Datasets for prefrontal areas*

We analyzed superficial-tissue hemodynamics in the prefrontal cortex using datasets from a previous study (exp. 1 to 2).[6] The datasets were measured for eight participants (mean age: 23.8 years) during a VFT using eight short channels in the prefrontal cortex. The task and channel positions are described in the previous studies.[6,44] In addition to the data obtained during the VFT, we also analyzed datasets obtained during a motor task from the same participants and using the same measurement locations. The motor task was a 15-s grasping task performed with the right hand and included a 30-s resting period after the task. Each session consisted of six trials. Only a single session was conducted for each participant. The sampling period was 100 ms for both sets of data.

A.1.3 *Results*

To estimate global superficial-tissue hemodynamics, we used PCA as in the analyses for exp. 1 and exp. 2 (see Sec. 2), except that high-pass filtering was set to a cutoff frequency of 0.003 Hz so as not to exclude task-related changes in the experiment with the long task duration (VFT). For motor tasks, task onset was defined as 1 s after the cue, as ball pressure levels or EMG data were not available. We observed similar transient increases in superficial-tissue hemodynamics (Fig. 5), which indicated that the first peak occurs ∼5 s after the task onset in all datasets. For task designs with long durations, the estimated superficial-tissue hemodynamics gradually increased again 10 s after the task onset and lasted until the end of the task. Thus, we confirm that the observed transient increase in superficial-tissue hemodynamics (Fig. 2) is task-design independent.

A.2 *Evaluation of Signal-to-Noise Ratio*

The SNRs for both ΔOxy- and ΔDeoxy-Hb were evaluated using a measure described by Erdoğan et al.[34] This measure is defined as the maximum amplitude after task onset divided by the standard deviation obtained during the pretask period (5 to 0 s before movement onset in this study). This is also referred to as the contrast-to-noise ratio.

We found that the SNR was 5.31 ± 1.60 (mean $\pm$ SD among participants) for ΔOxy-Hb($SNR_{\Delta Oxy}$), 2.95 ± 0.89 for ΔDeoxy-Hb ($SNR_{\Delta Deoxy}$), and 0.52 ± 0.61 for ΔDeoxy-Hb compared to that for ΔOxy-Hb ($SNR_{\Delta Deoxy}/SNR_{\Delta Oxy}$) among all the long channels. When we considered channels located at contralateral primary sensorimotor areas (channels 4, 6, 7, 9, 14, 15, 17, 18, and 19 for the left-hand task; and channels 24, 26, 27, 29, 34, 35, 36, 38, 39 for the right-hand task), we also found that the SNRs were 5.17 ± 1.75 ($SNR_{\Delta Oxy}$) and 3.07 ± 1.25 ($SNR_{\Delta Deoxy}$) and the ratio was <1 (0.69 ± 0.37). Thus, we confirmed that the SNR for ΔDeoxy-Hb was small compared to that for ΔOxy-Hb.

Disclosures

The authors declare no conflicts of interest.

Acknowledgments

This study was partly supported by the Japan Society of the Promotion Science Kakenhi Grant Nos. 2430051, 26560303, and 15K12597, Nagaoka University of Technology Presidential Research Grant, and the Strategic Research Program for Brain Science from MEXT of Japan. The authors would like to thank Hiroki Nakamura, Octavio Kazuyoshi Saito, and Yuta Oda for helping data collection.

References

1. D. T. Delpy et al., "Estimation of optical pathlength through tissue from direct time of flight measurement," *Phys. Med. Biol.* **33**(12), 1433–1442 (1988).
2. Y. Hoshi, "Functional near-infrared spectroscopy: potential and limitations in neuroimaging studies," *Int. Rev. Neurobiol.* **66**, 237–266 (2005).
3. M. Ferrari and V. Quaresima, "A brief review on the history of human functional near-infrared spectroscopy (fNIRS) development and fields of application," *Neuroimage* **63**(2), 921–935 (2012).
4. D. R. Leff et al., "Assessment of the cerebral cortex during motor task behaviours in adults: a systematic review of functional near infrared spectroscopy (fNIRS) studies," *Neuroimage* **54**(4), 2922–2936 (2011).
5. F. Scholkmann et al., "A review on continuous wave functional near-infrared spectroscopy and imaging instrumentation and methodology," *Neuroimage* **85**, 6–27 (2014).
6. T. Sato et al., "Reduction of global interference of scalp-hemodynamics in functional near-infrared spectroscopy using short distance probes," *Neuroimage* **141**, 120–132 (2016).
7. M. A. Franceschini et al., "Hemodynamic evoked response of the sensorimotor cortex measured noninvasively with near-infrared optical imaging," *Psychophysiology* **40**(4), 548–560 (2003).
8. I. Nambu et al., "Single-trial reconstruction of finger-pinch forces from human motor-cortical activation measured by near-infrared spectroscopy (NIRS)," *Neuroimage* **47**(2), 628–637 (2009).
9. K. Ishikuro et al., "Cerebral functional imaging using near-infrared spectroscopy during repeated performances of motor rehabilitation tasks tested on healthy subjects," *Front. Hum. Neurosci.* **8**, 2888 (2014).
10. Y. Ono et al., "Frontotemporal oxyhemoglobin dynamics predict performance accuracy of dance simulation gameplay: temporal characteristics of top-down and bottom-up cortical activities," *Neuroimage* **85**, 461–470 (2014).
11. H. Obrig et al., "Near-infrared spectroscopy: does it function in functional activation studies of the adult brain?," *Int. J. Psychophysiol.* **35**(2–3), 125–142 (2000).
12. R. P. Kennan et al., "Simultaneous recording of event-related auditory oddball response using transcranial near infrared optical topography and surface EEG," *Neuroimage* **16**(3), 587–592 (2002).
13. M. M. Plichta et al., "Model-based analysis of rapid event-related functional near-infrared spectroscopy (NIRS) data: a parametric validation study," *Neuroimage* **35**(2), 625–634 (2007).
14. M. M. Plichta et al., "Event-related functional near-infrared spectroscopy (fNIRS) based on craniocerebral correlations: reproducibility of activation?," *Hum. Brain Mapp.* **28**(8), 733–741 (2007).
15. M. L. Schroeter, S. Zysset, and D. Y. von Cramon, "Shortening intertrial intervals in event-related cognitive studies with near-infrared spectroscopy," *Neuroimage* **22**(1), 341–346 (2004).
16. T. Ikegami and G. Taga, "Decrease in cortical activation during learning of a multi-joint discrete motor task," *Exp. Brain Res.* **191**(2), 221–236 (2008).
17. Y. Sato et al., "Movement-related cortical activation with voluntary pinch task: simultaneous monitoring of near-infrared spectroscopy signals and movement-related cortical potentials," *J. Biomed. Opt.* **17**(7), 076011 (2012).
18. F. Scarpa et al., "A reference-channel based methodology to improve estimation of event-related hemodynamic response from fNIRS measurements," *Neuroimage* **72**, 106–119 (2013).
19. A. M. Dale and R. L. Buckner, "Selective averaging of rapidly presented individual trials using fMRI," *Hum. Brain Mapp.* **5**(5), 329–340 (1997).
20. R. Cunnington et al., "The preparation and readiness for voluntary movement: a high-field event-related fMRI study of the Bereitschafts-BOLD response," *Neuroimage* **20**(1), 404–412 (2003).
21. T. Aihara et al., "Cortical current source estimation from electroencephalography in combination with near-infrared spectroscopy as a hierarchical prior," *Neuroimage* **59**(4), 4006–4021 (2012).
22. H. Obrig et al., "Spontaneous low frequency oscillations of cerebral hemodynamics and metabolism in human adults," *Neuroimage* **12**(6), 623–639 (2000).
23. L. Minati et al., "Intra- and extra-cranial effects of transient blood pressure changes on brain near-infrared spectroscopy (NIRS) measurements," *J. Neurosci. Methods* **197**(2), 283–288 (2011).
24. E. Kirilina et al., "The physiological origin of task-evoked systemic artefacts in functional near infrared spectroscopy," *Neuroimage* **61**(1), 70–81 (2012).
25. E. Kirlilna et al., "Identifying and quantifying main components of physiological noise in functional near infrared spectroscopy on the prefrontal cortex," *Front. Hum. Neurosci.* **7**, 864 (2013).
26. G. E. Strangman, Q. Zhang, and Z. Li, "Scalp and skull influence on near infrared photon propagation in the Colin27 brain template," *Neuroimage* **85**, 136–149 (2014).
27. I. Tachtsidis and F. Scholkmann, "False positives and false negatives in functional near-infrared spectroscopy: issues, challenges, and the way forward," *Neurophotonics* **3**(3), 031405 (2016).
28. T. Yamada, S. Umeyama, and K. Matsuda, "Multidistance probe arrangement to eliminate artifacts in functional near-infrared spectroscopy," *J. Biomed. Opt.* **14**(6), 064034 (2009).
29. R. B. Saager, N. L. Telleri, and A. J. Berger, "Two-detector corrected near infrared spectroscopy (C-NIRS) detects hemodynamic activation responses more robustly than single-detector NIRS," *Neuroimage* **55**(4), 1679–1685 (2011).
30. L. Gagnon et al., "Improved recovery of the hemodynamic response in diffuse optical imaging using short optode separations and state-space modeling," *Neuroimage* **56**(3), 1362–1371 (2011).
31. T. Funane et al., "Quantitative evaluation of deep and shallow tissue layers' contribution to fNIRS signal using multi-distance optodes and independent component analysis," *Neuroimage* **85**, 150–165 (2014).
32. F. B. Haeussinger et al., "Reconstructing functional near-infrared spectroscopy (fNIRS) signals impaired by extra-cranial confounds: an easy-to-use filter method," *Neuroimage* **95**, 69–79 (2014).
33. X. Zhang, J. A. Noah, and J. Hirsch, "Separation of the global and local components in functional near-infrared spectroscopy signals using principal component spatial filtering," *Neurophotonics* **3**(1), 015004 (2016).
34. S. B. Erdoğan, M. A. Yücel, and A. Akın, "Analysis of task-evoked systemic interference in fNIRS measurements: insights from fMRI," *Neuroimage* **87**, 490–504 (2014).

35. Q. Zhang, E. N. Brown, and G. E. Strangman, "Adaptive filtering for global interference cancellation and real-time recovery of evoked brain activity: a Monte Carlo simulation study," *J. Biomed. Opt.* **12**(4), 044014 (2007).
36. M. Kiguchi and T. Funane, "Algorithm for removing scalp signals from functional near-infrared spectroscopy signals in real time using multi-distance optodes," *J. Biomed. Opt.* **19**(11), 110505 (2014).
37. T. Yamamoto et al., "Arranging optical fibres for the spatial resolution improvement of topographical images," *Phys. Med. Biol.* **47**(18), 3429–3440 (2002).
38. A. K. Singh et al., "Spatial registration of multichannel multi-subject fNIRS data to MNI space without MRI," *Neuroimage* **27**(4), 842–851 (2005).
39. K. J. Friston et al., *Statistical Parametric Mapping: The Analysis of Functional Brain Images*, 1st ed., Elsevier, Academic Press, Amsterdam, Boston (2007).
40. M. L. Seghier, "Laterality index in functional MRI: methodological issues," *Magn. Reson. Imaging* **26**(5), 594–601 (2008).
41. T. Yousry, "Localization of the motor hand area to a knob on the precentral gyrus. A new landmark," *Brain* **120**(1), 141–157 (1997).
42. J. C. Ye et al., "NIRS-SPM: statistical parametric mapping for near-infrared spectroscopy," *Neuroimage* **44**(2), 428–447 (2009).
43. A. K. Singh and I. Dan, "Exploring the false discovery rate in multi-channel NIRS," *Neuroimage* **33**(2), 542–549 (2006).
44. T. Takahashi et al., "Influence of skin blood flow on near-infrared spectroscopy signals measured on the forehead during a verbal fluency task," *Neuroimage* **57**(3), 991–1002 (2011).
45. R. B. Panerai et al., "Cerebral blood flow velocity response to induced and spontaneous sudden changes in arterial blood pressure," *Am. J. Physiol. Heart Circ. Physiol.* **280**(5), H2162–H2174 (2001).
46. M. Moody et al., "Cerebral and systemic hemodynamic changes during cognitive and motor activation paradigms," *Am. J. Physiol. Regul. Integr. Comp. Physiol.* **288**(6), R1581–R1588 (2005).
47. H. Tanaka, T. Katura, and H. Sato, "Task-related oxygenation and cerebral blood volume changes estimated from NIRS signals in motor and cognitive tasks," *Neuroimage* **94**, 107–119 (2014).
48. T. Funane et al., "Concurrent fNIRS-fMRI measurement to validate a method for separating deep and shallow fNIRS signals by using multidistance optodes," *Neurophotonics* **2**(1), 015003 (2015).
49. M. A. Yücel et al., "Mayer waves reduce the accuracy of estimated hemodynamic response functions in functional near-infrared spectroscopy," *Biomed. Opt. Express* **7**(8), 3078–3088 (2016).
50. L. Gagnon et al., "Short separation channel location impacts the performance of short channel regression in NIRS," *Neuroimage* **59**(3), 2518–2528 (2012).
51. Y. Zhang et al., "Multiregional functional near-infrared spectroscopy reveals globally symmetrical and frequency-specific patterns of superficial interference," *Biomed. Opt. Express* **6**(8), 2786–2802 (2015).

Isao Nambu received his PhD from Nara Institute of Science and Technology in 2010. Since 2012, he has been an assistant professor with Nagaoka University of Technology. His research interests include human motor control, motor learning, neuroimaging, and brain computer interfaces.

Takuya Ozawa received his ME in 2014 from Nagaoka University of Technology.

Takanori Sato received his BE and ME degrees from the Department of Electrical, Electronics, and Information Engineering, Nagaoka University of Technology, Nagaoka, Japan, in 2011 and 2013, respectively. Currently, he is a doctoral student in the course of integrated bioscience and technology at Nagaoka University of Technology. He has been engaged in research on functional near-infrared spectroscopy and brain–computer interfaces.

Takatsugu Aihara received his PhD from the University of Tokyo in 2010. Since 2009, he has been a researcher at the Advanced Telecommunications Research Institute International (ATR). His research interests include stochastic resonance in human brain, neuroimaging, and brain stimulation.

Yusuke Fujiwara: Biography is not available.

Yohei Otaka received his MD degree in 1997 and the PhD in 2016 from Keio University School of Medicine, Japan. From 2007 to 2011, he was a director of the Department of Rehabilitation Medicine in Tokyo Bay Rehabilitation Hospital. Since 2011, he has been working at the Department of Rehabilitation Medicine, Keio University School of Medicine. His research interests include neurorehabilitation, robotics, and fall prevention.

Rieko Osu received her PhD in Psychology at Kyoto University in 1996. From 1996 to 2001, she was a researcher for ERATO, JST. From 2001 to 2015, she worked as a researcher/senior researcher/department head of ATR Computational Neuroscience Laboratories. From 2015, she has been working as a director of consumer neuroscience, The Nielsen Company Japan. Her research interests are computational motor control, neuro-rehabilitation, as well as affective neuroscience.

Jun Izawa is an associate professor at the University of Tsukuba, Japan. His research interest is computational neuroscience and motor control.

Yasuhiro Wada received his BE, ME, and a PhD from Tokyo Institute of Technology. Currently, he is a professor at Nagaoka University of Technology. His research interests include network models, motor learning control, and brain computer interfaces.